ACS Synthetic Biology
Research Article
Cite This: ACS Synth. Biol. 2018, 7, 2647−2655
pubs.acs.org/synthbio

Highly Multiplexed CRISPRi Repression of Respiratory Functions Enhances Mitochondrial Localized Ethyl Acetate Biosynthesis in *Kluyveromyces marxianus*

Ann-Kathrin Löbs,[†] Cory Schwartz,[†] Sarah Thorwall,[†] and Ian Wheeldon*[,†,‡]

[†]Chemical and Environmental Engineering, University of California Riverside, Riverside, California 92521, United States
[‡]Center for Industrial Biotechnology, Bourns College of Engineering, University of California Riverside, Riverside, California 92521, United States

Supporting Information

ABSTRACT: The emergence of CRISPR-Cas9 for targeted genome editing and regulation has enabled the manipulation of desired traits and enhanced strain development of nonmodel microorganisms. The natural capacity of the yeast *Kluyveromyces marxianus* to produce volatile esters at high rate and at elevated temperatures make it a potentially valuable production platform for industrial biotechnology. Here, we identify the native localization of ethyl acetate biosynthesis in *K. marxianus* and use this information to develop a multiplexed CRISPRi system for redirecting carbon flux along central metabolic pathways, increasing ethyl acetate productivity. First, we identified the primary pathways of precursor and acetate ester biosynthesis. A genetic knockout screen revealed that the alcohol acetyltransferase Eat1 is the critical enzyme for ethyl, isoamyl, and phenylethyl acetate production. Truncation studies revealed that high ester biosynthesis is contingent on Eat1 mitochondrial localization. As ethyl acetate is formed from the condensation of ethanol and acetyl-CoA, we modulated expression of the TCA cycle and electron transport chain genes using a highly multiplexed CRISPRi approach. The simultaneous knockdown of *ACO2b*, *SDH2*, *RIP1*, and *MSS51* resulted in a 3.8-fold increase in ethyl acetate productivity over the already high natural capacity. This work demonstrates that multiplexed CRISPRi regulation of central carbon flux, supported by a fundamental understanding of pathway biochemistry, is a potent strategy for metabolic engineering in nonconventional microorganisms.

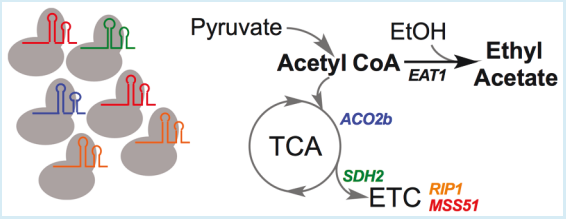

KEYWORDS: *AATase, CRISPR-Cas9, ester biosynthesis, gene regulation, metabolic engineering, thermotolerant yeast*

The advent of CRISPR-based technologies for targeted genome editing and regulation has rendered many nonconventional yeasts genetically accessible, a designation previously reserved for model organisms. One such model organism, the common yeast *Saccharomyces cerevisiae,* has proven to be a powerful tool in understanding eukaryotic genetics and is a successful synthetic biology host, but many nonconventional yeasts have native, polygenic traits that are desirable for industrial bioprocessing (e.g., stress tolerance) and have biosynthesis pathways that already produce high titers of valuable biochemicals.[1] However, manipulating expression levels of native and engineered pathways has been difficult due to a lack of standardized genetic parts and limited knowledge of their genetics and metabolism. Multiplexed CRISPR interference and activation (CRISPRi/a) systems help overcome this limitation by enabling precise transcriptional control and pathway optimization.[2−6]

The budding yeast *Kluyveromyces marxianus* is a good example of the benefits of nonconventional yeasts. It is thermotolerant to temperatures upward of 50 °C and can tolerate low pH.[1,7−9] A growth rate double that of *S. cerevisiae* is also beneficial for the production of growth-associated products[10] and is coupled with high TCA cycle flux and high intracellular pools of the central metabolite acetyl-CoA.[11] A native capacity for high rate ethyl acetate synthesis is also potentially valuable as a biochemical production route for short chain volatile esters. Wild-type strains have been shown to produce upward of 2 g L^{-1} h^{-1} in an aerated bioreactor on waste whey rich in galactose and lactose. Production rates on glucose, fructose, and to a lesser extent xylose are also high.[7]

Yeast ester biosynthesis is largely understood from genetic studies in *S. cerevisiae*. Double knockouts of alcohol acetyltransferases (AATases) *ATF1* and *ATF2* eliminate production of the medium chain ester isoamyl acetate and reduce ethyl acetate synthesis by ∼50%.[12] These and other AATases in *S. cerevisiae* (e.g., *EHT1*) first target to the endoplasmic reticulum (ER) and then traffic to lipid droplets, localization that is necessary for high activity.[13,14] The recent discovery of ethanol acetyltransferase (*EAT1*) in *Wickerhamomyces anomalus*, *S. cerevisiae*, and *K. marxianus*, among others, advanced our understanding of yeast ester biosynthesis.[15]

Received: August 2, 2018
Published: October 24, 2018

DOI: 10.1021/acssynbio.8b00331
ACS Synth. Biol. 2018, 7, 2647−2655

Disruption of *EAT1* in *S. cerevisiae* decreases ethyl acetate by 50%. Furthermore, heterologous overexpression of the *K. marxianus EAT1* homologue in *S. cerevisiae* resulted in high ethyl acetate production. In *K. marxianus*, ester synthesis is known to rely on the condensation of ethanol with acetyl-CoA in part through *ATF1* activity and likely through *EAT1* activity, although this has not yet been conclusively demonstrated.[10,16]

Here, we investigate *EAT1* as the primary biochemical route for ester biosynthesis and use a series of truncation studies to determine and control intracellular localization. These studies informed multiplexed CRISPRi modulation of central metabolic pathways to optimize the flux of key precursors to ethyl acetate and enhance biosynthesis. Six sgRNAs simultaneously targeted genes in the TCA cycle and electron transport chain (ETC) for repression, balancing ethanol and acetyl-CoA pools to increase ethyl acetate titer by 3.8-fold.

RESULTS

EAT1 Is the Primary Pathway for Ethyl, Isoamyl, and Phenylethyl Acetate Ester Biosynthesis. To identify the enzymatic pathways responsible for acetate ester production in *K. marxianus*, we created a series of genetic knockouts of genes with putative activity toward ester biosynthesis (Figure 1). The

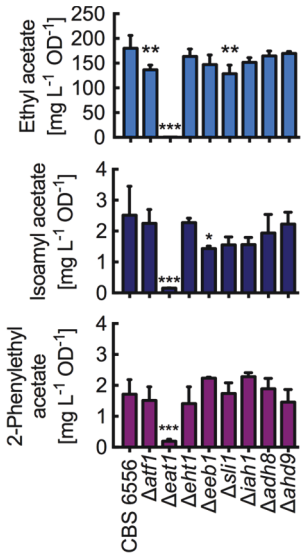

Figure 1. Genetic screening of ester biosynthesis in *K. marxianus*. CBS 6556 Δ*ura3* with a series of CRISPR-Cas9-induced disruptions to putative ester producing enzymes. Ester production was quantified after 10 h of shake flask culture in rich media (25 mL YPD in baffled shake flask) at 37 °C. Bars represent arithmetic mean with error bars indicating the standard deviation of biological replicates. Statistical significance was determined by one-way ANOVA with pairwise comparison to the CBS6556 control (*$p < 0.05$, **$p < 0.01$, and ***$p < 0.001$; $n \geq 3$ for all samples).

AATases *ATF1*, *EAT1*, *EHT1*, and *EEB1* were selected based on their annotation in the *K. marxianus* genome and homology to *S. cerevisiae* genes.[17,18] *SLI1* encodes for an N-acetyltransferase with possible activity toward ester biosynthesis.[19] *IAH1* is an isoamyl acetate esterase that may create esters via reverse esterase activity.[19] Finally, two putative alcohol dehydrogenase genes (*ADH8* and *ADH9*) were included for possible activity toward the conversion of intracellular hemiacetal to ethyl acetate.[10,20] Screening revealed that only knockout of *EAT1* significantly reduced ethyl, isoamyl, and phenylethyl acetate, reducing production by 99.6, 93.9, and 88.7%, respectively. The loss of ethyl acetate was accompanied by a significant accumulation of ethanol and acetaldehyde (Figure S1). Disruption of *ATF1* and *SLI1* also reduced ethyl acetate production (by 24 and 28.4%, respectively) but did not have a significant effect on the other esters.

Mitochondrial Localization of Eat1 Is Necessary for High Ethyl Acetate Production. On the basis of the gene disruption results, we expressed an integrated copy of *EAT1-GFP* and found that the fluorescent fusion protein colocalized with a red fluorescent mitochondrial stain (Figure 2A). Eat1 mitochondrial localization was also recently reported in *K. lactis*.[21] To identify the N-terminal domain responsible for targeting, we created a series of truncations and evaluated intracellular localization in both *S. cerevisiae* and *K. marxianus*. Truncations were based on transitions in the predicted secondary structure of the N-terminal domain (positions 6, 14, and 35[22]) and on a predicted cut site for a mitochondrial processing peptidase (position 19[23]). Heterologous expression in *S. cerevisiae* revealed that the wild-type sequence of Eat1 and Eat1 with truncation of the first 6 amino acids (Eat1(Δ1−6)-GFP) colocalized with a fluorescently tagged mitochondrial marker (OM45-DsRed; Figure S2). Mitochondrial localization was partially lost when the first 14 amino acids were removed with complete cytosolic expression resulting from truncation at the predicted cut site. Eat1(Δ1−14) and Eat1(Δ1−19) were subsequently expressed in *K. marxianus* with similar results: truncation prior to the cut site led to partial targeting, whereas removal of the first 19 amino acids resulted in cytosolic expression (Figure 2A and B).

Further analysis showed that mRNA and protein levels were consistent across the wild-type and truncation mutants (Figure 2C and D). However, ethyl acetate biosynthesis was significantly affected by altered intracellular localization. Overexpression of *EAT1* in *K. marxianus* with functional disruption to the native copy recovered ethyl acetate biosynthesis to 150 mg L^{-1} OD^{-1}, production equivalent to the wild-type strain (Figure 2E). Partial mitochondrial localization with Eat1(Δ1−14) reduced ethyl acetate production to 100 mg L^{-1} OD^{-1}, and cytosolic localization (Eat1(Δ1−19)) further decreased production to 45 mg L^{-1} OD^{-1}. Decreased ethyl acetate was accompanied by increased ethanol production (Figure S3). Kinetic analysis revealed that removal of the first 19 amino acids reduced activity, but the 14-amino acid truncation maintained wild-type reaction kinetics (Figure S4). This suggests that the loss in ethyl acetate biosynthesis is likely due to changes in localization and corresponding decreases in substrate availability (e.g., mitochondrial acetyl-CoA).

TCA Cycle and Electron Transport Chain (ETC) Genetic Targets for Modulating Ethyl Acetate Precursors. Previous *K. marxianus* culturing experiments have shown that chemical inhibition of the ETC can increase ethyl acetate biosynthesis.[16] Culturing under trace-metal limitations can also lead to an increase in ester production.[24] The hypothesis is that TCA cycle flux slows and acetyl-CoA accumulates when metal-dependent TCA enzymes have reduced activity and/or when the ETC is partially inhibited. Another potential consequence of ETC inhibition is the accumulation of reducing equivalents that are subsequently used to reduce pyruvate to ethanol.[16] This hypothesis led us to the following genetic targets to manipulate the ethyl acetate precursor pools of acetyl-CoA and

DOI: 10.1021/acssynbio.8b00331
ACS Synth. Biol. 2018, 7, 2647−2655

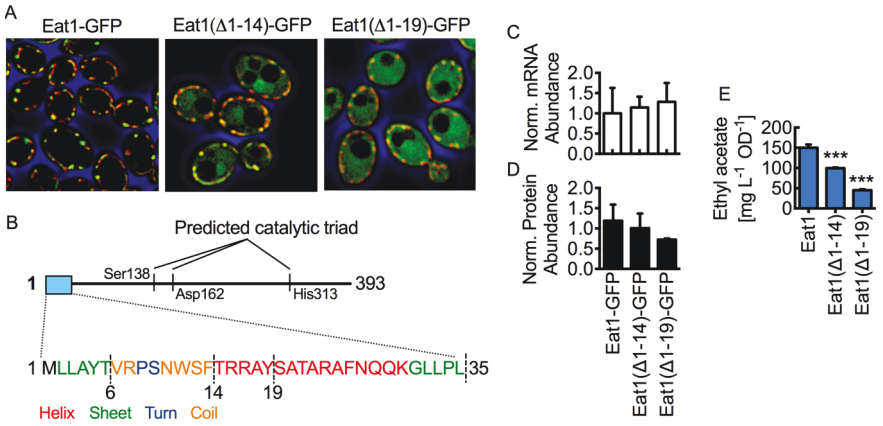

Figure 2. Intracellular localization of Eat1 in *K. marxianus*. (A) Fluorescence microscopy of *K. marxianus* expressing Eat1-GFP (green) variants with mitochondria identified by MitoTracker (red) fluorescence staining. Images were acquired using a 100× objective, and merged images of green fluorescence, red fluorescence, and phase contrast (blue) are shown. Yellow color indicates colocalization of red and green fluorescence. (B) Secondary structure and cut site prediction of the N-terminus of Eat1. (C) Quantification of transcript via qRT-PCR, and (D) protein levels via Western blot of GFP-tagged Eat1 and variants. (E) Ethyl acetate production from CBS 6556 Δ*ura3* Δ*eat1* expressing the wild-type sequence of Eat1 and two N-terminal truncations. Analysis was performed after 10 h of shake flask cultivation in rich media at 37 °C (25 mL of YPD in baffled shake flask). All bars represent arithmetic means of biological replicates, and error bars represent the standard deviation. Statistical significance was determined by one-way ANOVA with pairwise comparison to the wild-type Eat1 control (*$p < 0.05$, **$p < 0.01$, and ***$p < 0.001$; $n \geq 3$ for all samples).

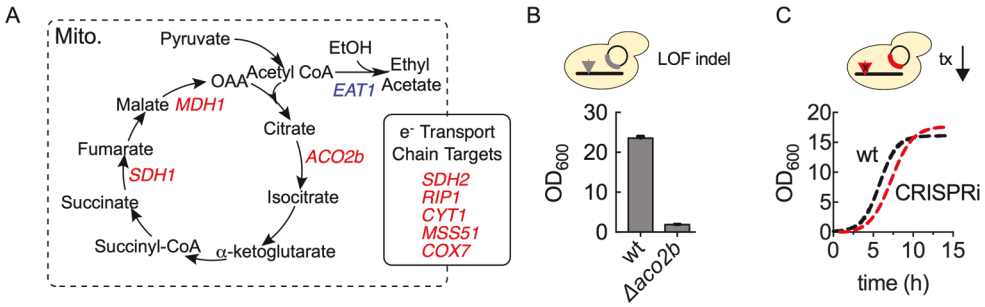

Figure 3. Target pathways for modulation of ethyl acetate biosynthesis precursors. (A) Partial diagram of ethyl acetate biosynthesis in *K. marxianus*. TCA cycle and electron transport chain (ETC) genes targeted for CRISPRi knockdown are identified in red. (B) *K. marxianus* CBS 6556 Δ*ura3* growth at 10 h with and without the functional disruption of *ACO2b* (25 mL of YPD in baffled shake flask, 37 °C). Bars represent the arithmetic mean, and error bars indicate the standard deviation. (C) Growth curves of CBS 6556 Δ*ura3* with and without constitutive expression of multiplexed CRISPRi knockdown of *ACO2b*, *SDH2*, *RIP1*, and *MSS51* from an episomal plasmid (25 mL of SD-U in baffled shake flask, 37 °C). The multiplexed CRISPRi sample shown here is characterized in Figure 5 and described in the Methods. For all samples, $n \geq 3$.

ethanol: aconitase (*ACO2b*), malate dehydrogenase (*MDH1*), succinate dehydrogenase subunits 1 and 2 (*SDH1* and *SDH2*), Rieske iron−sulfur protein (*RIP1*), heme-containing cytochrome c1 (*CYT1*), the transcriptional activator *MSS51*, and subunit 7 of cytochrome *c* oxidase (*COX7*; Figure 3A).

High biochemical production rates typically require high density cultures; as such, we targeted genetic knockdowns in place of functional gene disruptions to central metabolic pathways that may negatively affect cell growth. The chemical inhibition studies support this approach; biomass yields reduce to near zero levels with high ETC inhibition.[16] Genetic disruption of the TCA cycle produces a similar effect as evidenced by the knockout of *ACO2b* that resulted in severely limited growth (Figure 3B). Because genetic knockouts were not a viable strategy, we elected to repress the TCA cycle and ETC genes using CRISPR intereference (CRISPRi). CRISPRi uses a catalytically dead mutant of Cas9 (dCas9) to target the CRISPR-dCas9 complex to the promoter region of a gene. This targeting can suppress mRNA transcription by sterically blocking RNA polymerase II.[25] Multiplexed sgRNA expression enables the simultaneous targeting of multiple genomic loci.[2]

Here, we found that CRISPRi-mediated modulation of the TCA cycle and ETC functions did not significantly alter growth kinetics (Figure 3C).

Multiplexed CRISPRi for Transcriptional Regulation of Ethyl Acetate Biosynthesis. On the basis of our previous CRISPRi experience, we targeted two sgRNAs to each gene: one to a position close to the TATA box and a second close to the transcription start site (TSS).[2] Knockdown efficiencies were determined by qRT-PCR and compared to a nontargeting sgRNA control. Results showed that, with the exception of *CYT1*, all CRISPRi targeting resulted in a decrease in mRNA transcription (Figure 4A). Knockdown efficiencies ranged from 36% (*RIP1*) to 82% (*MDH1*). Although knockdowns were generally successful, only four of the suppressed genes resulted in increased ethyl acetate production. Knockdown of *ACO2b* increased ethyl acetate production from 48.3 mg L^{-1} OD^{-1} in the nontargeting control to 77.2 mg L^{-1} OD^{-1}. Suppression of *SDH2*, *RIP1*, and *MSS51* increased production to 67.1, 73.3, and 68.7 mg L^{-1} OD^{-1}, respectively (Figure 4A, bottom). In each case, ethanol production was not significantly affected (Figure S5). Of note

DOI: 10.1021/acssynbio.8b00331
ACS Synth. Biol. 2018, 7, 2647−2655

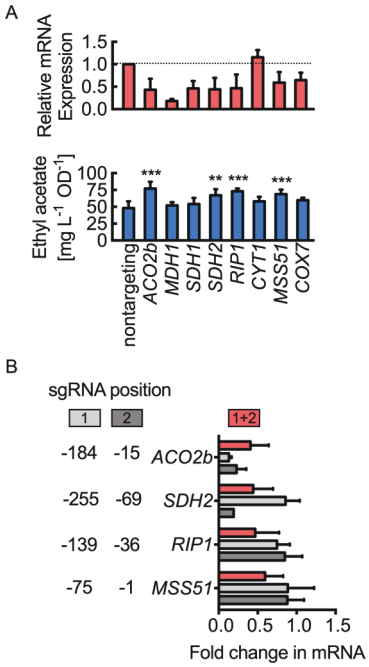

Figure 4. CRISPRi-mediated knockdown of TCA cycle and electron transport chain (ETC) genes increases ethyl acetate production. (A) Relative mRNA expression of targeted TCA cycle and ETC genes as measured by qRT-PCR relative to a sample expressing a nontargeting control (top). Each gene was modulated with an sgRNA targeted to the TATA box and a second sgRNA to the transcription start site (TSS). Knockdown of *ACO2b*, *SDH2*, *RIP1*, and *MSS51* increased ethyl acetate biosynthesis in comparison to a nontargeting sgRNA control (bottom). Cultures were grown in shake flasks to late exponential phase at 14 h in selective media to maintain the plasmid (50 mL of SD-U in baffled shake flask, 37 °C). (B) Effect of single- and dual-targeted sgRNAs on the transcription of *ACO2b*, *SDH2*, *RIP1*, and *MSS51*. The targeting position of each sgRNA relative to the start codon is shown on the left, and relative transcript level is shown on the right. Bars represent arithmetic means of at least three biological replicates, and error bars represent the standard deviation. Statistical significance for ethyl acetate production was determined by one-way ANOVA with pairwise comparison to the nontargeting control (*$p < 0.05$, **$p < 0.01$, and ***$p < 0.001$; $n \geq 3$ for all samples).

is that the CRISPRi experiments were conducted in synthetic-defined media without uracil (SD-U) to maintain expression of the plasmid-based system. A consequence of the media selection is reduced ethyl acetate in comparison to titers achieved in rich media (see Figures 1 and 2).

Simultaneous targeting of multiple genes requires highly multiplexed sgRNA expression; as such, we sought to understand the effect of each individual sgRNA on the suppression of the gene target. Figure 4B shows the position and effect of each sgRNA. For *ACO2b*, we found that singly targeted sgRNAs had a similar effect to dual targeting and that sgRNA 1 (localized to the TATA box; −184 relative to the start codon) resulted in the highest suppression level. Conversely, the sgRNA targeting close to the TSS of *SDH2* (position −69) was found to have a strong effect on expression, whereas sgRNA1 (position −255) had no effect. Both sgRNAs targeting the promoter regions of *RIP1* and *MSS51* were needed to achieve notable repression. These results were used to identify a six sgRNA multigene targeting approach to simultaneously modulate the TCA cycle and ETC in *K. marxianus* (Figure 5A).

The ethyl acetate and ethanol produced from all double and triple combinations of gene knockdowns along with the quadruple knockdown of *ACO2b*, *SDH2*, *RIP1*, and *MSS51* are shown in Figure 5B. Statistical analysis revealed a significant increase in ethyl acetate production for all knockdown combinations with the exception of the dual knockdown of *RIP1* and *MSS51*. Multigene targeting also increased ethyl acetate production compared to the single gene knockdowns shown in Figure 4A. The largest effects were observed with the triple combination of *ACO2b*, *SDH2*, and *MSS51*, which resulted in an increase of 2.18-fold, and when all four genes were suppressed, which increased ethyl acetate by 3.78-fold over the nontargeting control. With these two sgRNA combinations, ethanol biosynthesis was also significantly reduced by 1.67- and 2.85-fold, respectively. *K. marxianus* is often described as a Crabtree-negative yeast, but here and in previous work we observed ethanol production in aerobic cultures of engineered strains of *K. marxianus* CBS 6556.[10] Others have also reported ethanol production in aerobic cultures when glucose was used as the sole carbon source.[26] qRT-PCR analysis of the best strain where *ACO2b*, *SDH2*, *MSS51*, and *RIP1* were simultaneously targeted all showed knockdown efficiencies between 69 and 90% (Figure 5C). In this strain, all targets but *ACO2b* and *SDH2* showed a more efficient knockdown than when the individual genes were targeted. Taken together, these results demonstrate the transcriptional control of central respiratory metabolism via highly multiplexed CRISPRi transcriptional regulation to increase ethyl acetate biosynthesis.

DISCUSSION

Recent advancements in CRISPR-Cas9-based genome editing and transcriptional regulation tools have enabled rapid strain development of nonconventional yeasts for biochemical production.[1−3,6,10,27] Here, we advance these new synthetic biology tools by developing and applying a highly multiplexed CRISPRi strategy to modulate and enhance ethyl acetate biosynthesis in the yeast *K. marxianus*. This yeast was selected based on its high natural capacity to convert a range of pentose and hexose sugars into the short chain volatile ester ethyl acetate.[7] Thermotolerance to temperature upward of 50 °C and fast growth kinetics are also beneficial phenotypes for future translation to industrial processes.[1,9,10]

Prior to pathway engineering, we first needed to identify the enzymes responsible for ester biosynthesis. Previous work by our group and by others suggests that the condensation of ethanol with acetyl-CoA by AATase activity is the primary route to acetate ester biosynthesis in *K. marxianus*.[10,15,16] Knockout of the AATase *EAT1* confirmed this hypothesis; ethyl acetate biosynthesis was nearly eliminated, and isoamyl acetate and phenylethyl acetate production were reduced by over 88% (Figure 1). Localization studies of the Eat1 enzyme revealed mitochondrial targeting (Figure 2), behavior different from the well-studied *S. cerevisiae* AATases Atf1, Atf2, and Eht1, enzymes known to be responsible for the synthesis of various acetate esters.[13,28,29] Truncation of the first 19 amino acids of Eat1 eliminated the localization and resulted in cytosolic expression. Accompanying the altered localization was a significant reduction in ethyl acetate biosynthesis, most likely due to reduced acetyl-CoA availability in comparison

DOI: 10.1021/acssynbio.8b00331
ACS Synth. Biol. 2018, 7, 2647−2655

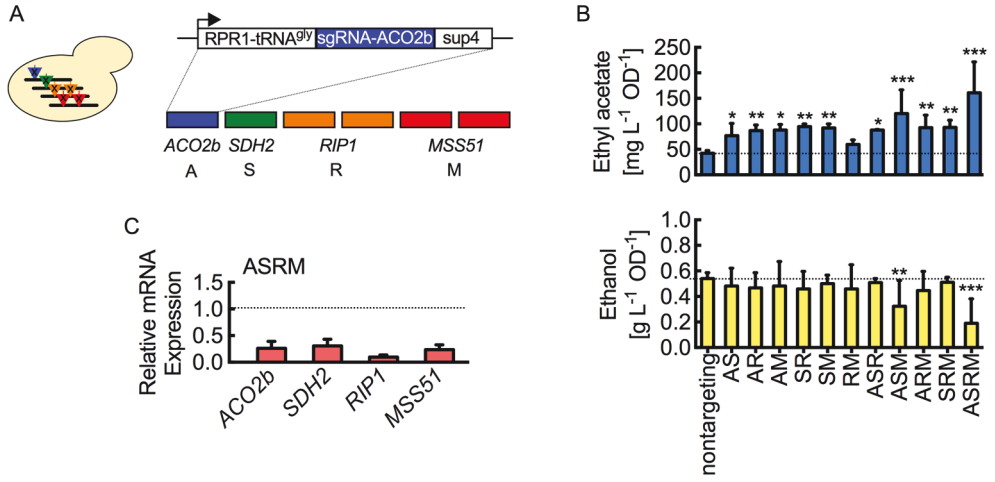

Figure 5. Highly multiplexed CRISRPi pathway tuning for enhanced ethyl acetate biosynthesis. (A) Schematic of multiplexed sgRNA expression. Each sgRNA was expressed from a unique cassette driven by a hybrid synthetic RNA polymerase III promoter with sup4 terminator. (B) Specific ethyl acetate and ethanol productivity from all double, triple, and quadruple targeting of *ACO2b*, *SDH2*, *RIP1*, and *MSS51* (A, S, R, and M, respectively). (C) Relative mRNA expression of *ACO2b*, *SDH2*, *RIP1*, and *MSS51* in strains with multiplexed targeting of *ACO2b*, *SDH2*, *RIP1*, and *MSS51* (ASRM) as measured by qRT-PCR. Relative expression is reported as the change relative to expression in the presence of a nontargeting control. Cultures were grown in shake flasks to late exponential phase at 14 h in selective media to maintain the plasmid (50 mL of SD-U in baffled shake flask, 37 °C). Statistical significance was determined by one-way ANOVA with pairwise comparison to the nontargeting control (*$p < 0.05$, **$p < 0.01$, and ***$p < 0.001$; $n \geq 3$ for all samples).

with the high native mitochondrial pool that is fueled by *K. marxianus*' fast growth kinetics.[11]

Given this new information, we targeted central respiratory pathways with the goal of enhancing the pool of mitochondrial acetyl-CoA available to Eat1 for ester biosynthesis. Previously published studies have shown that suppressing the ETC and TCA cycle through chemical inhibition and trace metal-limited media can increase ethyl acetate.[16,24] It has also been shown that under certain conditions iron limitation is necessary for the overproduction of ethyl acetate in various wild-type strains of *K. marxianus*.[30] Similar effects were observed in *Candida utiliz* and *C. pseudotropicalis*, where limited iron availability induced ester overproduction.[31−34] The hypothesis is that decreased flux through these pathways leads to an accumulation of acetyl-CoA and/or ethanol, precursors for ethyl acetate biosynthesis via AATase activity. Functional disruption of either the TCA cycle (Figure 3) or the ETC[35] drastically reduces aerobic growth, so an alternative strategy was needed. As such, we elected to genetically test this hypothesis through CRISPRi repression targeting the TCA genes *ACO2b*, *MDH1*, and *SDH1* and ETC genes *SDH2, RIP1*, *CYT1*, *MSS51*, and *COX7*. The iron−sulfur cluster containing Aco2b catalyzes the second step of the TCA cycle, converting citrate to isocitrate. The Sdh2 enzyme is responsible for transferring electrons from succinate to ubiquinone; the Rip1 protein is essential to ETC complex III activity by oxidizing ubiquinol and transferring electrons to cytochromes *c*1 and *b*566; and, Mss51 is essential for assembly and translational activation of the cytochrome oxidase subunit 1 (*COX1*), which is one of three core subunits of ETC complex IV.[36−38] The CRISPRi screen was successful in repressing all but *CYT1* with repression of *ACO2b*, *SDH2*, *RIP1*, and *MSS51* resulting in increased ethyl acetate (Figure 4).

A highly multiplexed CRISRPi screen targeting all double and triple combinations of *ACO2b*, *SDH2*, *RIP1*, and *MSS51* as well as the simultaneous suppression of all four genes was performed using the most effective sgRNAs for each gene target. This combinatorial screen used up to six sgRNAs each expressed from a separate cassette driven by a hybrid synthetic RNA polymerase III promoter in a single plasmid for multiplexed expression.[10,39] The quadruple knockdown was most effective in increasing the already high native specific production of ethyl acetate by 3.78-fold and decreasing ethanol by 2.84-fold. These results demonstrate that the CRISPRi approach was successful in modulating the central metabolic pathways that generate the precursor to ethyl acetate. Increased ethyl acetate production accompanied by decreased ethanol suggests that we were successful in increasing carbon flux to the mitochondrial pool of acetyl-CoA but also that this pool is limiting for ester biosynthesis. We furthermore demonstrate that up to six sgRNAs can be simultaneously expressed without a detrimental impact to knockdown efficiencies (Figure 5C).

We note that the effectiveness of CRISPRi knockdown was variable. In some cases, knockdown was efficient, whereas in others, significant transcriptional repression was not observed (Figure 4A). Similar results have been reported elsewhere and can be attributed to differences in the ability of a given sgRNA to target dCas9 to the loci of interest and to a positional effect within the promoter.[2,3,40] It is likely that both of these effects contribute to the variation in CRISPRi efficiency between the two sgRNAs targeted to each promoter (Figure 3B). Multiplexing can also contribute to the observed variation. For example, multiplexing had a slightly detrimental effect on *ACO2b* and *SDH2* knockdown (87 and 81% knockdown with single sgRNAs vs 74 and 69% knockdown in multiplexed format; compare Figures 4B and 5C). In these cases, it is possible that knockdown efficiency was limited by Cas9 or sgRNA expression levels. Another possibility is that changes in metabolism due to targeted gene suppression alter the transcription level of other targeted genes. That is to say that the baseline transcriptional levels of all targeted genes may be effected by the knockdown of one or more of *ACO2b*, *SDH2*, *RIP1*, and *MSS51*. The fact that *MSS51* and *RIP1* repression appeared to be stronger when targeted in multiplexed mode could be a result of decreased expression caused by a decrease

DOI: 10.1021/acssynbio.8b00331
ACS Synth. Biol. 2018, 7, 2647−2655

in flux through the TCA cycle and ETC. Further experiments are needed to confirm this hypothesis.

The nonconventional yeast *K. marxianus* is a promising eukaryotic host for chemical biosynthesis. Similar to other nonconventional yeasts, our current understanding of its metabolism and genetics is limited in comparison with our knowledge of the common yeast *S. cerevisiae*. In this work, we developed and used advanced CRISPR-based genome editing and regulation tools to identify *EAT1* as the primary route for acetate ester biosynthesis and genetically modulated precursor pathways to enhance production. Identifying mitochondrial localization of the Eat1 enzyme was critical as it revealed a possible explanation as to why *K. marxianus* natively produces ethyl acetate at high rates (i.e., enzyme colocalization with high concentrations of acetyl-CoA compartmentalized in the mitochondria) and provided targets for pathway manipulations to enhance production. With a highly multiplexed CRISPRi system, we demonstrate that gene regulation in nonconventional yeasts can be readily manipulated to control phenotypes of interest and amplify native traits that are well-suited to industrial biotechnology.

METHODS

Strains and Culturing Conditions. All strains were purchased from ATCC or DSMZ strain collections. All materials were purchased from Fisher Scientific unless noted otherwise. All yeast strains used in this study are listed in Table S1. This list includes *K. marxianus* CBS 6556 Δ*ura3* (YS402), which was used as the control strain (see ref 10) and *S. cerevisiae* strain BY4742 (YS5) with DSRED-tagged OM45, which was used to study mitochondrial localization.

For creating knockout strains of *K. marxianus,* cells were transformed with a CRISPR-Cas9 plasmid and grown on SD-U containing 6.7 g L^{-1} yeast nitrogen base without amino acids DB Difco (Becton-Dickinson), 1.92 g L^{-1} yeast synthetic drop-out medium supplements without uracil (Sigma-Aldrich), and 20 g L^{-1} glucose or SD-U plates containing 15 g L^{-1} agar. For removing the CRISPR-Cas9 plasmid, cells were grown in YPD medium (5 g L^{-1} yeast extract, 10 g L^{-1} peptone with 20 g L^{-1} glucose; DB Difco) overnight. *K. marxianus* CRISPRi cultures were grown in 50 mL of SD-U media in 250 mL baffled shake flasks (0.2 initial OD_{600}) at 250 rpm and 37 °C for 14 h (late exponential phase). Initial and final optical cell densities (OD_{600}) were measured using the Nanodrop 2000c UV−vis spectrometer (ThermoFisher Scientific) at 600 nm. *K. marxianus* disruption and *EAT1* integration strains (see Table S1) were cultured in YPD media (5 g L^{-1} yeast extract, 10 g L^{-1} peptone with 20 g L^{-1} glucose; DB Difco) at 37 °C. Overnight cultures were inoculated into 25 mL of media in 250 mL baffled shake flasks.

Molecular Cloning and Plasmids Construction. All cloning was accomplished using Q5 polymerase, restriction endonucleases, and HiFi DNA assembly master mix purchased from New England BioLabs (NEB). DNA oligos were purchased from Integrated DNA Technologies (IDT). Chemically competent DH5α *Escherichia coli* was used for plasmid propagation. Following transformation, *E. coli* cells were grown in LB medium containing 100 mg L^{-1} ampicillin. All plasmids and primers used are listed in Tables S2 and S3.

To construct a version of the Cas9 nuclease lacking nuclease activity (dCas9), two point mutations (D10A and H840A) were introduced as described earlier.[25] pIW601 was digested with *Xma*I/AvrII and assembled with two dCas9 fragments containing the two mutations necessary (Figure S6) that were amplified from pIW601 with P1853/54 and P1855/56, yielding pIW602. The sgRNA-containing CRISPR-Cas9 and -dCas9 plasmids were constructed using pIW601 (Addgene ID 98907) and pIW602, respectively. For integration of the 20 bp target sequence, pIW601 or pIW602 was digested with PspXI and assembled with a 60 bp cassette containing 20 bp upstream and downstream homology as well as the target sequence. The cassette was constructed by annealing two complementary 60 bp primers as previously described.[39] Target sequences were checked for secondary structure using the IDT OligoAnalyzer Tool 3.1 (https://www.idtdna.com/calc/analyzer) and uniqueness within the *K. marxianus* genome using BLAST. All sgRNA sequences and primers are listed in Tables S3 and S4. Cas9/dCas9 expression was driven by a constitutive *S. cerevisiae TEF1* promoter, and sgRNA expression was governed by a synthetic polymerase III promoter as described earlier.[10]

S. cerevisiae EAT1 overexpression plasmids were constructed by amplifying *EAT1*, and the truncations with AL276, AL280−283, and AL277 (Table S3) and cloned into pRS426 vector containing a PGK1 expression cassette (pIW21). For genomic integration into the *URA3* locus, a homology donor plasmid was constructed. The marker of pIW272 was exchanged for *S. cerevisiae HIS3* by assembling the amplified backbone and the *HIS3* marker amplified from plasmid pIW8. The resulting plasmid pIW578 was digested to insert 1 kb upstream and downstream homology donors, respectively. Expression cassettes for genomic integration (amplified from genomic DNA using AL47/116 AL49/117) were inserted into the cut pIW578 to generate pIW634 (Tables S2 and S3). *E. coli EAT1* and *EAT1* truncation expression plasmids were cloned by digesting pet28b PspXI/NcoI and Hifi Assembly of appropriate *EAT1* inserts that were amplified from the *K. marxianus* genome using the appropriate primers (Table S3). For cloning CRISPRi plasmids expressing sgRNAs targeting multiple genes, plasmids targeting a single gene were digested with AvrII or NsiI. Cassettes expressing additional sgRNAs were amplified via PCR (for example, with Cr_1539 and Cr_1540) and cloned into the digested backbone using Hifi Assembly as has been previously described.[2]

Transformation of *K. marxianus* and *S. cerevisiae*. Plasmid and linear DNA transformations were performed as previously described.[10] Briefly, *K. marxianus* cells were grown to stationary phase, washed with sterile water, and suspended in 100 μg of carrier DNA (salmon sperm DNA) and 0.2−1 μg of plasmid or linear DNA. Then, 400 μL of transformation mix (40% polyethylene glycol 3350, 0.1 M lithium acetate, 10 mM Tris-HCl (pH 7.5), 1 mM EDTA, and 10 mM DTT) was added, and the solution was incubated at room temperature for 15 min and subsequently heat shocked at 47 °C for 15 min. The transformed cells were plated on solid SD-U agar plates. *S. cerevisiae* cells were transformed using the Frozen-EZ Yeast Transformation II Kit (Zymo Research) and plated on solid SD-U agar plates.

Strain Construction. For gene disruptions, transformed *K. marxianus* cells were plated on SD-U plates and grown for 2 days at 30 °C. After 2 days of growth, colonies were screened by amplifying the CRISPR-Cas9-edited region in the genome by colony PCR and subsequent sequencing of the purified PCR fragments. The native *OM45* gene of *S. cerevisiae* BY4742 (YS5) was fused to *DSRED* by homologous recombination to create a mitochondrial marker strain (YS578). For genomic

DOI: 10.1021/acssynbio.8b00331
ACS Synth. Biol. 2018, 7, 2647−2655

integrations, *K. marxianus* CBS6556 Δ*ura3* was transformed with a CRISPR plasmid (pIW538) and a homology donor plasmid and plated on SD-U plates. After 2 days of growth at 30 °C, colonies were picked and restreaked on YPD plates. The resulting colonies were subjected to colony PCR using a three-primer approach as described before.[41] In brief, two primers binding outside of the homology region (P1928/29) and in the promoter (AL275) were used for PCR, where a 2 kb band represents no integration through homologous recombination and a 1.2 kb band corresponds to genomic integration of the expression cassette at the *URA3* site. Positively confirmed disruptions or integrations were grown overnight in YPD liquid cultures for plasmid removal and saved at −80 °C.

Eat1 Protein Sequence Analysis. The Eat1 protein sequenced was analyzed for secondary structures using the CFSSP software.[22] On the basis of the structure analysis, truncations were made at residues 6, 14, 18, and 35. Mitochondrial localization was assessed using the MitoFates software.[23]

Headspace Gas Chromatography. For GC analysis, 1 mL of culture supernatant was used for headspace GC analysis in a 10 mL headspace vial containing 1 g of NaCl. Volatile metabolite concentration was measured using an Agilent 7890A system equipped with a Phenomenex ZB-624 column and an FID detector. For metabolite separation, the temperature was held at 40 °C for 2 min and then increased 20 °C min^{-1} to 70 and 50 °C min^{-1} to 220 °C and held for 2 min. For calculating metabolite concentrations, standard curves for ethyl acetate, ethanol, isoamyl acetate, and 2-phenylethyl acetate were created by spiking various amounts of metabolite into the appropriate media (YPD or SD-U) containing 1 g of NaCl. It is worth noting that cultures for ester production were performed in shake flasks covered by foil that allow for gas transfer. Therefore, measured ethyl acetate concentrations may not reflect the total amount of ester synthesized due to possible losses through ester evaporation.

Reverse Transcription Quantitative PCR (qRT-PCR). Total RNA was extracted as described before.[10] In short, RNA was extracted from 5 OD of cells using the YeaStar RNA Kit (Zymo Research). Following DNase treatment (DNase I, New England Biolabs), RNA was purified using the RNA Clean & Concentrator-5 Kit (Zymo Research). RNA was subjected to reverse transcription (iScript Reverse Transcription Supermix for qRT-PCR), and cDNA was used for SYBR Green qPCR (SsoAdvanced Universal SYBR Green Supermix) using the CFX Connect Real Time PCR Detection System (BioRad). Primers used for the qRT-PCR reaction are listed in Table S3. Fold changes in mRNA relative to a nontargeting control were calculated using the Pfaffl method, taking into account the reaction efficiency as previously described and normalized to *ACT1* expression.[42]

MitoTracker Staining. For Eat1 localization studies, *K. marxianus* cultures with an integrated copy of *EAT1-GFP* and its truncations (see Table S1) were grown overnight in YPD media and transferred to fresh media (OD 0.1). Five hundred microliters of cells were harvested, resuspended in fresh media with 100 nM MitoTracker Red CMXRos (Cell Singaling Technology), and incubated at 37 °C for 15 min. Subsequently, the cells were washed twice, resuspended in media, and imaged immediately.

Fluorescence Microscopy. *S. cerevisiae* and stained *K. marxianus* cells were imaged with an Olympus BX51 microscope (UPlanFL 100× 1.30 oil-immersion objective lens, mercury lamp), and fluorescent images were captured by a Q-Imaging Retiga Exi CCD camera. Images were processed using CellSens Dimension 1.7 software (Olympus).

Western Blot Analysis. Western blot analysis was done to quantify protein translation of the Eat1-GFP fusion protein and its truncations in *K. marxianus*. Then, 2.5 OD of cells were lysed and loaded onto a 10-well Any kD Mini-PROTEAN TGX Precast Protein Gel (BioRad) and run for 1 h at 150 V.[10] Samples were then electrophoretically transferred overnight to a PVDF membrane at 25 V. Membranes were blocked with 5% nonfat milk in Tris-buffered saline (TBST, 20 mM Tris-base, 150 mM NaCl) with 0.05% Tween20) for 1 h at room temperature and incubated with rabbit anti-GFP antibody (NB600-303; Novus Biologicals) or mouse anti-GAPDH (PA1-987; Fisher Scientific) diluted to 1:2000 and 1:5000 in TBST buffer with 1% nonfat milk. Goat antirabbit (65-6120, Invitrogen) and antimouse IgG-HRP (31430; Fisher Scientific) diluted to 1:10000 were added as secondary antibodies and incubated at room temperature for 30 min. After washing with TBST, the Immobilon Western Chemiluminescent HRP substrate (Millipore) was used for signal detection. Blots were imaged, and protein levels were quantified using the ChemiDoc MP System with the Image Lab software (BioRad).

Protein Expression and Purification. Eat1 and its two truncations were expressed using *E. coli* T7 Express lysY cells (New England Biolabs) transformed with the respective expression plasmids pIW1019-21 (Table S2). Shake flasks of LB media with 50 $\mu g\ mL^{-1}$ of kanamycin sulfate were inoculated with 8 mL of overnight culture per liter of media. Cultures were grown for ∼4 h at 30 °C and 200 rpm. At an OD_{600} of 0.3−0.5, cultures were induced with 0.2 mM IPTG and incubated overnight at 25 °C and 200 rpm. Cells were spun down at 5000*g* for 10 min, and pellets were washed with 50 mM potassium phosphate buffer, pH 7.4 and stored at −80 °C. Thawed cell pellets were resuspended in 25 mL of wash buffer (50 mM potassium phosphate buffer, 300 mM NaCl, pH 8.0) per liter of culture. Cells were lysed by sonication (3 s on, 7 s off) for 10 min on ice using a sonicator (Thermo Fisher Scientific). Lysate was spun down for 35 min at 15,000*g*, and the resulting soluble fraction was filtered through a 0.45 μm filter. Proteins were purified by nickel affinity chromatography and size exclusion chromatography using a BioLogic DuoFlow FPLC system (BioRad) with a QuadTec UV−vis detector and fraction collector. Clarified lysate was run through a 5 mL HisTrap HP column (GE Healthcare Life Sciences), and the protein was eluted in steps. The column was washed with 50 mM KP_i, 300 mM NaCl, 50 mM imidazole, pH 8.0, and protein was eluted with 50 mM KP_i, 300 mM NaCl, 250 mM imidazole, pH 8.0. Fractions containing the Eat1 enzyme were concentrated and buffer exchanged using 30 kDa Amicon Ultra centrifuge filters (EMD Millipore) according to the manufacturer's instructions. The resulting 0.5 mL sample was run through a Superdex 200 Increase 10/300 GL column (GE Healthcare Life Sciences) equilibrated with 50 mM Tris, 150 mM NaCl, pH 7.4 buffer. Fractions were analyzed using SDS PAGE, and proteins were quantified using A_{280} values collected from a NanoDrop 2000c spectrophotometer (Thermo Fisher Scientific) and extinction coefficients calculated from ExPASy ProtParam.

Enzyme Kinetics. The AATase activity assay is based off the methods by Kruis et al.[15] Fifty-μL reactions were set up in a clear, flat-bottom 96-well plate (Thermo Fisher Scientific)

DOI: 10.1021/acssynbio.8b00331
ACS Synth. Biol. 2018, 7, 2647−2655

corresponding to different acetyl-coA concentrations and time points. Each reaction contained 40 mM ethanol, 10 μM respective Eat1 enzyme, and assay buffer (50 mM Tris, 150 mM NaCl, pH 7.4). Reactions were initiated at 10 min time points by adding varying amounts of acetyl-CoA (0−4 mM). After the reactions had progressed for the desired amount of time, 40 μL of each was transferred to its corresponding measuring well in another clear, flat-bottom 96-well plate containing 0.25 mM 5,5′-dithibis-2-nitrobenzoic acid (DTNB) and assay buffer for a final volume of 200 μL per well. The absorbance at 412 nm was measured immediately using a Synergy 4 plate reader (BioTek). The slopes of the absorbance data, 14150 M^{-1} cm^{-1} $TNB2^-$ extinction coefficient, and 0.3 cm path length were used to calculate the initial reaction rate. The slopes of the absorbance data and the apparent Michaelis−Menten constants were calculated with linear and nonlinear regression, respectively, using Graphpad Prism 6 software.

Statistical Analysis. Data points represent arithmetic means of at least triplicate biological samples, and error bars represent the standard deviation. Groups of samples were analyzed by one-way ANOVA with Dunnett's multiple comparison when appropriate ($*p < 0.05$, $**p < 0.01$, and $***p < 0.001$; $n \geq 3$ for all samples). Statistical analysis and plotting of data points was performed using GraphPad Prism software.

■ ASSOCIATED CONTENT

Supporting Information

The Supporting Information is available free of charge on the ACS Publications website at DOI: 10.1021/acssynbio.8b00331.

Supplementary data figures supporting main manuscript, dCas9 protein sequence, tables of strains, plasmids, and primers, and sgRNA sequences used in this work (PDF)

■ AUTHOR INFORMATION

Corresponding Author

*E-mail: iwheeldon@engr.ucr.edu.

ORCID

Ian Wheeldon: 0000-0002-3492-7539

Author Contributions

A.K.L. and I.W. conceived the study and designed the experiments. A.K.L. and C.S. completed the CRISPRi screen. S.T. and I.W. completed the enzyme kinetic analysis. All other experiments were performed by A.K.L. All authors analyzed the data and wrote the manuscript.

Notes

The authors declare no competing financial interest.

■ ACKNOWLEDGMENTS

This work was supported by NSF 1510697 and 1803630 and by DOE DE-SC0019093.

■ REFERENCES

(1) Löbs, A. K., Schwartz, C., and Wheeldon, I. (2017) Genome and metabolic engineering in non-conventional yeasts: Current advances and applications. *Synth. Syst. Biotechnol. 2* (3), 198−207.

(2) Schwartz, C., Frogue, K., Ramesh, A., Misa, J., and Wheeldon, I. (2017) CRISPRi repression of nonhomologous end-joining for enhanced genome engineering via homologous recombination in *Yarrowia lipolytica*. *Biotechnol. Bioeng. 114* (12), 2896−2906.

(3) Schwartz, C., Curtis, N., Lobs, A. K., and Wheeldon, I. (2018) Multiplexed CRISPR Activation of Cryptic Sugar Metabolism Enables *Yarrowia Lipolytica* Growth on Cellobiose. *Biotechnol. J. 13* (9), No. e1700584.

(4) Farzadfard, F., Perli, S. D., and Lu, T. K. (2013) Tunable and Multifunctional Eukaryotic Transcription Factors Based on CRISPR/Cas. *ACS Synth. Biol. 2* (10), 604−613.

(5) Zalatan, J. G., Lee, M. E., Almeida, R., Gilbert, L. A., Whitehead, E. H., La Russa, M., Tsai, J. C., Weissman, J. S., Dueber, J. E., Qi, L. S., and Lim, W. A. (2015) Engineering Complex Synthetic Transcriptional Programs with CRISPR RNA Scaffolds. *Cell 160* (1−2), 339−350.

(6) Cao, M., Gao, M., Ploessl, D., Song, C., and Shao, Z. (2018) CRISPR-mediated Genome Editing and Gene Repression in *Scheffersomyces stipitis*. *Biotechnol. J. 13*, No. e1700598.

(7) Löbs, A. K., Lin, J. L., Cook, M., and Wheeldon, I. (2016) High throughput, colorimetric screening of microbial ester biosynthesis reveals high ethyl acetate production from Kluyveromyces marxianus on C5, C6, and C12 carbon sources. *Biotechnol. J. 11* (10), 1274−1281.

(8) Urit, T., Loser, C., Wunderlich, M., and Bley, T. (2011) Formation of ethyl acetate by Kluyveromyces marxianus on whey: studies of the ester stripping. *Bioprocess Biosyst. Eng. 34* (5), 547−559.

(9) Fonseca, G. G., Heinzle, E., Wittmann, C., and Gombert, A. K. (2008) The yeast Kluyveromyces marxianus and its biotechnological potential. *Appl. Microbiol. Biotechnol. 79* (3), 339−54.

(10) Löbs, A. K., Engel, R., Schwartz, C., Flores, A., and Wheeldon, I. (2017) CRISPR-Cas9-enabled genetic disruptions for understanding ethanol and ethyl acetate biosynthesis in *Kluyveromyces marxianus*. *Biotechnol. Biofuels 10*, 164.

(11) Blank, L. M., Lehmbeck, F., and Sauer, U. (2005) Metabolic-flux and network analysis in fourteen hemiascomycetous yeasts. *FEMS Yeast Res. 5* (6−7), 545−558.

(12) Verstrepen, K. J., Van Laere, S. D. M., Vanderhaegen, B. M. P., Derdelinckx, G., Dufour, J. P., Pretorius, I. S., Winderickx, J., Thevelein, J. M., and Delvaux, F. R. (2003) Expression levels of the yeast alcohol acetyltransferase genes ATF1, Lg-ATF1, and ATF2 control the formation of a broad range of volatile esters. *Appl. Environ. Microbiol. 69* (9), 5228−5237.

(13) Lin, J. L., and Wheeldon, I. (2014) Dual N- and C-Terminal Helices Are Required for Endoplasmic Reticulum and Lipid Droplet Association of Alcohol Acetyltransferases in Saccharomyces cerevisiae. *PLoS One 9* (8), e104141.

(14) Zhu, J., Lin, J. L., Palomec, L., and Wheeldon, I. (2015) Microbial host selection affects intracellular localization and activity of alcohol-O-acetyltransferase. *Microb. Cell Fact. 14*, 35.

(15) Kruis, A. J., Levisson, M., Mars, A. E., van der Ploeg, M., Garces Daza, F., Ellena, V., Kengen, S. W. M., van der Oost, J., and Weusthuis, R. A. (2017) Ethyl acetate production by the elusive alcohol acetyltransferase from yeast. *Metab. Eng. 41*, 92−101.

(16) Loser, C., Urit, T., Keil, P., and Bley, T. (2015) Studies on the mechanism of synthesis of ethyl acetate in *Kluyveromyces marxianus* DSM 5422. *Appl. Microbiol. Biotechnol. 99* (3), 1131−44.

(17) Lertwattanasakul, N., Kosaka, T., Hosoyama, A., Suzuki, Y., Rodrussamee, N., Matsutani, M., Murata, M., Fujimoto, N., Suprayogi, Tsuchikane, K., Limtong, S., Fujita, N., and Yamada, M. (2015) Genetic basis of the highly efficient yeast *Kluyveromyces marxianus*: complete genome sequence and transcriptome analyses. *Biotechnol. Biofuels 8*, 47.

(18) Saerens, S. M. G., Verstrepen, K. J., Van Laere, S. D. M., Voet, A. R. D., Van Dijck, P., Delvaux, F. R., and Thevelein, J. M. (2006) The Saccharomyces cerevisiae EHT1 and EEB1 genes encode novel enzymes with medium-chain fatty acid ethyl ester synthesis and hydrolysis capacity. *J. Biol. Chem. 281* (7), 4446−4456.

(19) Gethins, L., Guneser, O., Demirkol, A., Rea, M. C., Stanton, C., Ross, R. P., Yuceer, Y., and Morrissey, J. P. (2015) Influence of carbon and nitrogen source on production of volatile fragrance and flavour metabolites by the yeast *Kluyveromyces marxianus*. *Yeast 32* (1), 67−76.

DOI: 10.1021/acssynbio.8b00331
ACS Synth. Biol. 2018, 7, 2647−2655

(20) Inokuma, K., Ishii, J., Hara, K. Y., Mochizuki, M., Hasunuma, T., and Kondo, A. (2015) Complete Genome Sequence of Kluyveromyces marxianus NBRC1777, a Nonconventional Thermotolerant Yeast. *Genome Announc. 3* (2), e00389-15.
(21) Kruis, A. J., Mars, A. E., Kengen, S. W. M., Borst, J. W., van der Oost, J., and Weusthuis, R. A. (2018) The alcohol acetyltransferase Eat1 is located in yeast mitochondria. *Appl. Environ. Microbiol.*, 1.
(22) Kumar, T. A. (2013) CFSSP: Chou and Fasman Secondary Structure Prediction server. *Wide Spectrum 1* (9), 15−19.
(23) Fukasawa, Y., Tsuji, J., Fu, S. C., Tomii, K., Horton, P., and Imai, K. (2015) MitoFates: Improved Prediction of Mitochondrial Targeting Sequences and Their Cleavage Sites. *Mol. Cell. Proteomics 14* (4), 1113−1126.
(24) Urit, T., Stukert, A., Bley, T., and Loser, C. (2012) Formation of ethyl acetate by *Kluyveromyces marxianus* on whey during aerobic batch cultivation at specific trace element limitation. *Appl. Microbiol. Biotechnol. 96* (5), 1313−23.
(25) Smith, J. D., Suresh, S., Schlecht, U., Wu, M., Wagih, O., Peltz, G., Davis, R. W., Steinmetz, L. M., Parts, L., and St Onge, R. P. (2016) Quantitative CRISPR interference screens in yeast identify chemical-genetic interactions and new rules for guide RNA design. *Genome Biol. 17*, 45.
(26) Fonseca, G. G., de Carvalho, N. M. B., and Gombert, A. K. (2013) Growth of the yeast Kluyveromyces marxianus CBS 6556 on different sugar combinations as sole carbon and energy source. *Appl. Microbiol. Biotechnol. 97* (11), 5055−5067.
(27) Schwartz, C., Frogue, K., Misa, J., and Wheeldon, I. (2017) Host and Pathway Engineering for Enhanced Lycopene Biosynthesis in Yarrowia lipolytica. *Front. Microbiol. 8*, 2233.
(28) Lin, J. L., Zhu, J., and Wheeldon, I. (2016) Rapid ester biosynthesis screening reveals a high activity alcohol-O-acyltransferase (AATase) from tomato fruit. *Biotechnol. J. 11* (5), 700−707.
(29) Knight, M. J., Bull, I. D., and Curnow, P. (2014) The yeast enzyme Ehtl is an octanoyl-CoA:ethanol acyltransferase that also functions as a thioesterase. *Yeast 31* (12), 463−474.
(30) Loser, C., Urit, T., Stukert, A., and Bley, T. (2013) Formation of ethyl acetate from whey by Kluyveromyces marxianus on a pilot scale. *J. Biotechnol. 163* (1), 17−23.
(31) Thomas, K. C., and Dawson, P. S. (1978) Relationship between iron-limited growth and energy limitation during phased cultivation of Candida utilis. *Can. J. Microbiol. 24* (4), 440−7.
(32) Armstrong, D. W., and Yamazaki, H. (1984) Effect of Iron and Edta on Ethyl-Acetate Accumulation in Candida-Utilis. *Biotechnol. Lett. 6* (12), 819−824.
(33) Willetts, A. (1989) Ester formation from ethanol by Candida pseudotropicalis. *Antonie van Leeuwenhoek 56* (2), 175−80.
(34) Corzo, G., Revah, S., and Christen, P. (1995) Effect of oxygen on the ethyl acetate production from continuous ethanol stream by Candida utilis in submerged cultures. *Dev. Food Sci. 37*, 1141−1141.
(35) Merz, S., and Westermann, B. (2009) Genome-wide deletion mutant analysis reveals genes required for respiratory growth, mitochondrial genome maintenance and mitochondrial protein synthesis in *Saccharomyces cerevisiae*. *Genome Biol. 10* (9), R95.
(36) Siep, M., van Oosterum, K., Neufeglise, H., van der Spek, H., and Grivell, L. A. (2000) Mss51p, a putative translational activator of cytochrome c oxidase subunit-1 (COX1) mRNA, is required for synthesis of Cox1p in *Saccharomyces cerevisiae*. *Curr. Genet. 37* (4), 213−220.
(37) Oyedotun, K. S., and Lemire, B. D. (2004) The quaternary structure of the Saccharomyces cerevisiae succinate dehydrogenase - Homology modeling, cofactor docking, and molecular dynamics simulation studies. *J. Biol. Chem. 279* (10), 9424−9431.
(38) Graham, L. A., and Trumpower, B. L. (1991) Mutational Analysis of the Mitochondrial Rieske Iron-Sulfur Protein of Saccharomyces-Cerevisiae 0.3. Import, Protease Processing, and Assembly into the Cytochrome-Bc1 Complex of Iron-Sulfur Protein Lacking the Iron-Sulfur Cluster. *J. Biol. Chem. 266* (33), 22485−22492.
(39) Schwartz, C. M., Hussain, M. S., Blenner, M., and Wheeldon, I. (2016) Synthetic RNA Polymerase III Promoters Facilitate High-Efficiency CRISPR-Cas9-Mediated Genome Editing in *Yarrowia lipolytica*. *ACS Synth. Biol. 5* (4), 356−359.
(40) Deaner, M., and Alper, H. S. (2017) Systematic testing of enzyme perturbation sensitivities via graded dCas9 modulation in *Saccharomyces cerevisiae*. *Metab. Eng. 40*, 14−22.
(41) Schwartz, C., Shabbir-Hussain, M., Frogue, K., Blenner, M., and Wheeldon, I. (2017) Standardized Markerless Gene Integration for Pathway Engineering in *Yarrowia lipolytica*. *ACS Synth. Biol. 6* (3), 402−409.
(42) Pfaffl, M. W. (2001) A new mathematical model for relative quantification in real-time RT-PCR. *Nucleic Acids Res. 29* (9), No. e45.

DOI: 10.1021/acssynbio.8b00331
ACS Synth. Biol. 2018, 7, 2647−2655